2024 European Control Conference (ECC)
June 25-28, 2024. Stockholm, Sweden

VC-EKF for Graphical Nonlinear Systems

Simeng Guo[1], Wenling Li[1], Bin Zhang[2] and Yang Liu[1]

Abstract— This paper investigates the issue of extended Kalman filtering (EKF) for graphical nonlinear systems. For the signals that have a nonlinear relationship with the graph Laplacian matrix, we introduce a variance-constrained (VC)-EKF, leveraging the graph Fourier transform (GFT), aimed at enhancing the filtering performance. In this paper, the GFT is applied for system variables and the updated estimate is designed with a diagonal gain matrix for the transformed system, then the higher-order terms are introduced into the predicted error and the updated error, and the diagonal gain matrix can be acquired through the solution of two Riccati-like equations. The advantages of the GFT-VC-EKF are that, the gain matrix represented by a diagonal matrix enables the node signal to be updated independently, thus reducing the iterative cumulative error, and the introduction of higher-order terms makes it possible to compensate for the linearization error caused by the fact that the EKF containing only first-order Taylor expansion term. A simulation example on a power system proves the superiority of the proposed filter.

Index Terms— Variance-constrained, Extended Kalman filter, Laplacian matrix, Graph Fourier transform.

I. Introduction

The filtering problem in graphical systems is widely applicable across diverse domains, including but not limited to image processing [1], social network [2], recommender systems [3], multi-agent systems [4], and sensor networks [5]. In order to improve the filtering accuracy, scholars have designed various filters for the graphical systems [6]–[8].

For the time-invariant graphical systems, the core idea of graph signal processing (GSP) has been adopted by the existing literature to describe, transform, and process the signal to realize the recovery, reconstruction, or estimation [9], [10]. For instance, the problem of optimal Wiener filtering on graphs was extended to fractional Fourier domains in [11], showing promise for enhancing performance by reducing errors. A sample domain discrete trigonometric transform (DTT) filter implementation was introduced in [12], drawing upon the designs of polynomial graph filters and designs involving multivariate polynomials in graph filtering. However, practical engineering is usually modeled as time-varying graphical systems in the field of control, so the design of dynamic filters for time-varying graphical systems has become an important research direction.

The processing of time-invariant graphical systems provides new tools for the filtering of time-varying graphical systems, such as graph filter [13], graph recognition [14], and graph Fourier transform (GFT) [15]. Using the above tools, some filters for graphical nonlinear systems have been developed [16], [17]. In [16], a novel approach to unscented Kalman filtering (UKF) based on graphs was introduced. This approach leveraged the graph Laplacian matrix to design the Kalman gain matrix, enabling independent updates for each vertex signal. However, the above literature only discussed the case where the measurement output is related to the graph topology. The literature [17] made up for the above shortcomings, and developed a GSP-extended Kalman filter (EKF) for the system where both the monitoring target and the measurement output are related to the graph topology. The GSP-EKF was designed with a diagonal gain matrix through the transformation of the EKF into the graph frequency domain. However, there is a linearization error due to the fact that the EKF only retains the first-order Taylor expansion term, which makes the filtering accuracy of the GSP-EKF still has some room for improvement.

Building upon the preceding discussion, this paper focus on designing a GFT-variance-constrained (VC)-EKF for graphical nonlinear systems from two aspects: Compensating for the linearization error and reducing the iterative cumulative error. Specifically, we first decompose the graph Laplacian matrix and use the eigenvector matrix to apply the GFT for the variables in the monitoring target and measurement output. Based on this, the gain matrix can be designed as a diagonal matrix following the structure of the graph filter, so that the node signal can be updated independently. Next, the higher-order terms containing bounded time-varying matrix are introduced into the transformed predicted and updated error to compensate for the linearization error. Finally, the diagonal gain matrix can be determined by solving a pair of transformed Riccati-like equations. Simulation results on a power system show that the proposed GFT-VC-EKF has better performance.

The organization of the following sections in this paper is as outlined below. Section II gives the definition of a graphical nonlinear system and presents the problem to be solved. Section III details the design of the GFT-VC-EKF. Section IV presents a numerical example on a power system, followed by discussions on conclusions

* This work was supported by NSFC (62376015, U22B2038, 62073020).

[1] Simeng Guo, Wenling Li, and Yang Liu are with the School of Automation Science and Electrical Engineering, Beihang University (BUAA), Beijing 100191, China gsmeng@buaa.edu.cn; lwlmath@buaa.edu.cn; ylbuaa@163.com

[2] Bin Zhang is with the School of Artificial Intelligence, Beijing University of Posts and Telecommunications, Beijing 100876, China zhangbinzdh@bupt.edu.cn

and future work in Section V.

Notation: The identity matrix I is defined with appropriate dimensions, while A^T denotes the transpose of matrix A. For symmetric matrices A and B, if $A > B\,(A \geq B)$, then $A - B$ is positive definite (positive semidefinite).

II. Problem Formulation

This paper establishes the topology structure of nonlinear systems using an undirected graph denoted as $\mathcal{G} = (\mathcal{V}, \mathcal{E}, A)$. In this context, $\mathcal{V}$ denotes the collection of nodes, while $\mathcal{E} \in \mathcal{V} \times \mathcal{V}$ signifies the interconnected edges among these nodes. The representation of connections between nodes is captured by the adjacency matrix, $A = [a_{ij}]_{N\times N}$, where each entry a_{ij} is non-negative. Within the framework of this adjacency matrix, the element at position (i, j) signifies the existence of an edge between the ith and jth nodes; specifically, $a_{ij} > 0$ if (i, j) belongs to $\mathcal{E}$. Additionally, it is assumed in this paper that the diagonal entries satisfy $a_{ii} = 1$.

The Laplacian matrix of the undirected graph, denoted as $L = D - A$, involves D representing the degree matrix of the given graph. Its eigenvalue decomposition, $L = V\Lambda V^T$, includes V as the matrix of eigenvectors and Λ as the eigenvalue matrix. Specifically, $VV^T = I$, and Λ is diagonal. By defining the Laplacian matrix L as a graph shift operator (GSO), a graph filter $g\,(L)$ is established. This graph filter $g\,(L)$ can be further decomposed into

$$g\,(L) = V g\,(\Lambda)\, V^T \tag{1}$$

where $g\,(\cdot)$ is a function, and $g\,(\Lambda)$ is a diagonal matrix.

Consider the following graphical nonlinear systems:

$$x_{k+1} = f(L, x_k) + w_k \tag{2}$$

and the measurement signals

$$z_k = h(L, x_k) + v_k \tag{3}$$

where $x_k = \begin{bmatrix} x_{1,k} & x_{2,k} & \dots & x_{N,k} \end{bmatrix}^T \in \mathbf{R}^N$ and $z_k \in \mathbf{R}^N$ represent the status of the monitoring target and the measurement signals, respectively. $f\,(\cdot)$ represents a nonlinear function, while $h\,(\cdot)$ denotes a measurement function. We make the assumption that w_k and v_k are independent sequences of Gaussian white noise, both characterized by zero mean and covariance matrices Q and R, respectively. Fig. 1 illustrates the model of graphical nonlinear systems.

This paper aims to develop a filter to improve the filtering performance specifically for graphical nonlinear systems in terms of compensating the linearization error and reducing the iterative accumulative error.

The introduction of the following lemmas is essential for deriving the primary results of this paper.

Lemma 1 [18]: Assuming $\Pi = \Pi^T > 0$ and a scalar $\delta > 0$ satisfying $\delta^{-1} I > \Omega\Pi\Omega^T$, we have the following matrix inequality

$$\begin{aligned}(\Phi + \Xi\Psi\Omega)\,\Pi(\Phi + \Xi\Psi\Omega)^T \\ \leq \Phi\left(\Pi^{-1} - \delta\Omega^T\Omega\right)^{-1}\Phi^T + \delta^{-1}\Xi\Xi^T\end{aligned}$$

where Φ, Ξ, Ψ, and Ω are matrices with appropriate dimensions and satisfy $\Psi\Psi^T \leq I$.

Lemma 2 [19]: Assuming $0 \leq k < n$ and $P = P^T > 0$, let $\phi_k\,(\cdot)$ and $\vartheta_k\,(\cdot)$ represent two sequences of matrix functions as given in

$$\phi_k\,(P) = \phi_k\left(P^T\right), \vartheta_k\,(P) = \vartheta_k\left(P^T\right)$$

If a matrix $Q = Q^T > P$ exists as described in

$$\phi_k\,(Q) \geq \phi_k\,(P), \vartheta_k\,(Q) \geq \phi_k\,(Q)$$

then the solutions, denoted as Φ_k and Ξ_k, to the subsequent difference equations:

$$\Phi_k = \phi_k\,(\Phi_{k-1}), \Xi_k = \vartheta_k\,(\Xi_{k-1}), \Phi_0 = \Xi_0 > 0$$

meet the condition $\Phi_k \leq \Xi_k$.

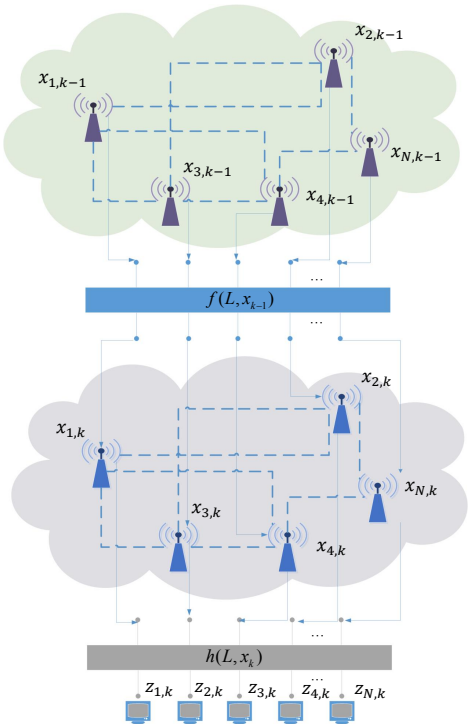

Fig. 1. Graphical nonlinear systems.

III. Main Results

We first define the GFT of the node signal on the graphical nonlinear systems by using the eigenvector matrix as

$$\begin{aligned}x_k^v = V^T x_k, f^v(L, x_k^v) = V^T f(L, x_k), w_k^v = V^T w_k \\ z_k^v = V^T z_k, h^v(L, x_k^v) = V^T h(L, x_k), v_k^v = V^T v_k\end{aligned}$$

then we can derive the transformed system as outlined below:

$$x_{k+1}^v = f^v(L, x_k^v) + w_k^v \tag{4}$$

$$z_k^v = h^v(L, x_k^v) + v_k^v \tag{5}$$

Next, we design the filter for the above system.

Assuming that the updated estimate $\hat{x}^v_{k|k}$ and the updated filtering error covariance matrix $P^v_{k|k}$ are known at time k, let the predicted estimate of x^v_{k+1} at time k be

$$\hat{x}^v_{k+1|k} = f^v\left(L, \hat{x}^v_{k|k}\right) \tag{6}$$

then the one step predicted filtering error is represented by means of

$$\begin{aligned}\tilde{x}^v_{k+1|k} &= x^v_{k+1} - \hat{x}^v_{k+1|k} \\ &= f^v\left(L, x^v_k\right) - f^v\left(L, \hat{x}^v_{k|k}\right) + w^v_k\end{aligned} \tag{7}$$

By utilizing a Taylor series expansion for the system transition function $f^v(\cdot)$ centered at $\hat{x}^v_{k|k}$, we can obtain the following expression

$$f^v\left(L, x^v_k\right) = f^v\left(L, \hat{x}^v_{k|k}\right) + F^v_k \tilde{x}^v_{k|k} + o\left(\left|\tilde{x}^v_{k|k}\right|\right) \tag{8}$$

where $F^v_k = \left.\frac{\partial f^v(L, x^v_k)}{\partial x^v_k}\right|_{x^v_k = \hat{x}^v_{k|k}}$ is the Jacobian matrix, and the higher-order term can be denoted as

$$o\left(\left|\tilde{x}^v_{k|k}\right|\right) = U^v_k \Omega^v_k \tilde{x}^v_{k|k} \tag{9}$$

where U^v_k is a given problem-dependent scaling matrix and Ω^v_k is a time-varying matrix accounting for the linearization error satisfying $\Omega^v_k \Omega^{vT}_k \leq I$.

Then the one step predicted filtering error (7) can be characterized by the following expression

$$\tilde{x}^v_{k+1|k} = \left(F^v_k + U^v_k \Omega^v_k\right) \tilde{x}^v_{k|k} + w^v_k \tag{10}$$

and the corresponding filtering error covariance matrix can be calculated as

$$P^v_{k+1|k} = \left(F^v_k + U^v_k \Omega^v_k\right) P^v_{k|k} \left(F^v_k + U^v_k \Omega^v_k\right)^T + Q^v \tag{11}$$

where $Q^v = V^T Q V$.

Next, let the updated estimate at time $k+1$ be

$$\hat{x}^v_{k+1|k+1} = \hat{x}^v_{k+1|k} + K^v_{k+1}\left[z^v_{k+1} - h^v\left(L, \hat{x}^v_{k+1|k}\right)\right] \tag{12}$$

where K^v_{k+1} is the gain matrix to be determined.

Remark 1: In this step, we design the gain matrix K_{k+1} in the EKF as a graph filter $g_{k+1}(L)$ designed by the GSO L, then the gain matrix K^v_{k+1} in (12) can be a diagonal matrix. Specifically, the updated estimate in the EKF is denoted by

$$\hat{x}_{k+1|k+1} = \hat{x}_{k+1|k} + K_{k+1}\left[z_{k+1} - h\left(L, \hat{x}_{k+1|k}\right)\right] \tag{13}$$

which is equivalent to the following equation

$$\begin{aligned}V\hat{x}^v_{k+1|k+1} &= V\hat{x}^v_{k+1|k} + V K^v_{k+1} V^T \\ &\quad \times \left[V z^v_{k+1} - V h^v\left(L, \hat{x}^v_{k+1|k}\right)\right]\end{aligned} \tag{14}$$

then it is obviously that $K_{k+1} = V K^v_{k+1} V^T$. It can be seen from (1) that, $K^v_{k+1} = g_{k+1}(\Lambda)$ which means K^v_{k+1} is designed as a diagonal matrix. It has been shown in [16] and [17] that, the advantage of designing the gain matrix as a diagonal matrix is that the algorithm does not need to solve for the inverse of the non-diagonal matrix at each time step, and the signal of each node can be updated independently, so that the accumulation of filtering errors can be reduced.

Similarly, by employing a Taylor series expansion for the measurement transition function $h^v(\cdot)$ centered at $\hat{x}^v_{k+1|k}$, the following expression can be obtained

$$\begin{aligned}h^v\left(L, x^v_k\right) &= h^v\left(L, \hat{x}^v_{k+1|k}\right) + H^v_{k+1}\tilde{x}^v_{k+1|k} \\ &\quad + o\left(\left|\tilde{x}^v_{k+1|k}\right|\right)\end{aligned} \tag{15}$$

where $H^v_{k+1} = \left.\frac{\partial h^v(L, x^v_k)}{\partial x^v_k}\right|_{x^v_k = \hat{x}^v_{k+1|k}}$. The higher-order term can be described by $o\left(\left|\tilde{x}^v_{k+1|k}\right|\right) = S^v_{k+1}\Pi^v_{k+1}\tilde{x}^v_{k+1|k}$. Here, S^v_{k+1} denotes a scaling matrix that depends on the specific problem, and Π^v_{k+1} accounts for time-varying factors, addressing the presence of linearization errors, which remains unknown and must satisfy $\Pi^v_{k+1}\Pi^{vT}_{k+1} \leq I$.

Then the updated filtering error can be given by

$$\begin{aligned}\tilde{x}^v_{k+1|k+1} &= x^v_{k+1} - \hat{x}^v_{k+1|k+1} \\ &= \left[I - K^v_{k+1}\left(H^v_{k+1} + S^v_{k+1}\Pi^v_{k+1}\right)\right] \\ &\quad \times \tilde{x}^v_{k+1|k} - K^v_{k+1} v^v_{k+1}\end{aligned} \tag{16}$$

and the corresponding covariance matrix results from

$$\begin{aligned}P^v_{k+1|k+1} &= \left[I - K^v_{k+1}\left(H^v_{k+1} + S^v_{k+1}\Pi^v_{k+1}\right)\right] \\ &\quad \times P^v_{k+1|k}\left[I - K^v_{k+1}\left(H^v_{k+1}\right.\right. \\ &\quad \left.\left. + S^v_{k+1}\Pi^v_{k+1}\right)\right]^T + K^v_{k+1} R^v K^{vT}_{k+1}\end{aligned} \tag{17}$$

where $R^v = V^T R V$.

To deal with the unknown matrices Ω^v_k and Π^v_{k+1}, we solve for the gain matrix K^v_{k+1} through determining the upper bound of the covariance matrices $P^v_{k+1|k}$ and $P^v_{k+1|k+1}$.

Theorem 1: Consider the graphical nonlinear system after transformation, as described by (4) and (5), and introduce two positive scalars α^v_k and β^v_k. If the subsequent pair of Riccati-like difference equations:

$$\begin{aligned}\Phi^v_{k+1|k} &= F^v_k\left(\left(\Phi^v_{k|k}\right)^{-1} - \alpha^v_k I\right)^{-1} F^{vT}_k \\ &\quad + \left(\alpha^v_k\right)^{-1} U^v_k U^{vT}_k + Q^v\end{aligned} \tag{18}$$

$$\begin{aligned}\Phi^v_{k+1|k+1} &= \left(I - K^v_{k+1} H^v_{k+1}\right) \\ &\quad \times \left(\left(\Phi^v_{k+1|k}\right)^{-1} - \beta^v_k I\right)^{-1} \\ &\quad \times \left(I - K^v_{k+1} H^v_{k+1}\right)^T \\ &\quad + K^v_{k+1}\left(\left(\beta^v_k\right)^{-1} S^v_{k+1} S^{vT}_{k+1} + R^v\right) \\ &\quad \times K^{vT}_{k+1}\end{aligned} \tag{19}$$

have positive definite solutions, labeled as $\Phi^v_{k+1|k}$ and $\Phi^v_{k+1|k+1}$, with an initial condition $\Phi^v_{0|0} = P^v_{0|0} > 0$ and satisfying the subsequent inequalities for all $k \geq 0$

$$\begin{aligned}\left(\alpha^v_k\right)^{-1} I &> \Phi^v_{k|k} \\ \left(\beta^v_k\right)^{-1} I &> \Phi^v_{k+1|k}\end{aligned}$$

then the matrix $\Phi^v_{k+1|k+1}$ signifies an upper bound of $P^v_{k+1|k+1}$. Furthermore, the diagonal gain matrix K^v_{k+1} is restricted as

$$\begin{aligned} K^v_{k+1} = ddiag &\left(\left(\left(\Phi^v_{k+1|k} \right)^{-1} - \beta^v_k I \right)^{-1} H^{vT}_{k+1} \right) \\ &\times \left(ddiag \left(H^v_{k+1} \left(\left(\Phi^v_{k+1|k} \right)^{-1} - \beta^v_k I \right)^{-1} \right. \right. \\ &\left. \left. \times H^{vT}_{k+1} + (\beta^v_k)^{-1} S^v_{k+1} S^{vT}_{k+1} + R^v \right) \right)^{-1} \end{aligned} \tag{20}$$

where $ddiag\,(\cdot)$ signifies a diagonal matrix composed of the diagonal elements extracted from the matrix in parentheses.

Proof. Applying Lemma 1 to (11) and (17), we have

$$\begin{aligned} P^v_{k+1|k} \le F^v_k &\left(\left(P^v_{k|k} \right)^{-1} - \alpha^v_k I \right)^{-1} F^{vT}_k \\ &+ (\alpha^v_k)^{-1} U^v_k U^{vT}_k + Q^v \end{aligned} \tag{21}$$

$$\begin{aligned} P^v_{k+1|k+1} \le &\left(I - K^v_{k+1} H^v_{k+1} \right) \\ &\times \left(\left(P^v_{k+1|k} \right)^{-1} - \beta^v_k I \right)^{-1} \\ &\times \left(I - K^v_{k+1} H^v_{k+1} \right)^T \\ &+ K^v_{k+1} \left((\beta^v_k)^{-1} S^v_{k+1} S^{vT}_{k+1} + R^v \right) \\ &\times K^{vT}_{k+1} \end{aligned} \tag{22}$$

Then, by applying Lemma 2 to (11), (17), (21), and (22), it becomes evident that

$$\begin{aligned} P^v_{k+1|k} &\le \Phi^v_{k+1|k} \\ P^v_{k+1|k+1} &\le \Phi^v_{k+1|k+1} \end{aligned} \tag{23}$$

Finally, the gain matrix can be determined by setting the following equation to zero

$$\begin{aligned} \frac{\partial tr\left(\Phi^v_{k+1|k+1} \right)}{\partial K^v_{k+1}} = &-2 \left(\left(\Phi^v_{k+1|k} \right)^{-1} - \beta^v_k I \right)^{-1} H^{vT}_{k+1} \\ &+ 2K^v_{k+1} \left[H^v_{k+1} \right. \\ &\times \left(\left(\Phi^v_{k+1|k} \right)^{-1} - \beta^v_k I \right)^{-1} H^{vT}_{k+1} \\ &\left. + \left((\beta^v_k)^{-1} S^v_{k+1} S^{vT}_{k+1} + R^v \right) \right] \end{aligned} \tag{24}$$

Up to now, the design of the GFT-VC-EKF is complete. □

Remark 2: It is well known that, the EKF using the first expansion term of Taylor series has obvious linearization error. Although the higher-order EKF can make the system parameters closer to the original nonlinear relationship, the calculation is more complicated. To eliminate the linearization error easily, the VC approach was put forward in [20], and the advantage of the VC approach used in EKF has been proved in various models [21]–[23]. Different from the above literature, the objective of this paper is to enhance the filtering accuracy of the VC-EKF even further.

IV. Numerical Simulation

In this section, the advantages of the GFT approach are verified and GFT-VC-EKF is compared with existing filters.

We employ the graphical dynamic model to depict the state transition and the measurement output in the power system [24]. The state vector x_k encompasses the voltage phases of various buses, while the measurement output z_k includes the active powers at these buses. The electrical network's structure is determined by the Laplacian matrix L [25].

The function $f(\cdot)$ is denoted by $f(L, x_k) = cos(x_k)$, and the measurement function $h(\cdot)$ is represented by

$$\begin{aligned} [h(L, x_k)]_i = \sum_{j=1}^{N} &|e_i| \, |e_j| \, (G_{i,j} \cos(x_{i,k} - x_{j,k}) \\ &+ B_{i,j} \sin(x_{i,k} - x_{j,k})) \end{aligned} \tag{25}$$

where $x_{i,k}$ represents the voltage phase at the ith bus, while $|e_i|$ denotes its amplitude. The parameters $G_{i,j}$ and $B_{i,j}$ correspond to the conductance and susceptance of the transmission line linking buses i and j, respectively, where $(i, j) \in \mathcal{E}$ [26]. In normalized power systems, it is a common assumption to set $|e_i| = 1$ [26]. Additionally, we set $G_{i,j}$ to a value of 10.

The graph representation of the electrical network, denoted by L, is typically associated with the susceptance of the transmission lines $B_{i,j}$ [27], and their relations are constructed as:

$$L = \begin{cases} -B_{i,j}, & i \neq j \\ \sum\limits_{c=1, c \neq i}^{N} B_{i,c}, & i = j \end{cases} \tag{26}$$

The associated Jacobian matrix is derived by (25) as:

$$\begin{aligned} &[H(L, x_k)]_{i,j} = \frac{\partial h_i(L, x_k)}{\partial x_k} = \\ &\begin{cases} G_{i,j} \sin(x_{i,k} - x_{j,k}) \\ \qquad - B_{i,j} \cos(x_{i,k} - x_{j,k}), & i \neq j \\ \sum\limits_{c=1, c \neq i}^{N} -G_{i,c} \sin(x_{i,k} - x_{c,k}) \\ \qquad + B_{i,c} \cos(x_{i,k} - x_{c,k}), & i = j \end{cases} \end{aligned} \tag{27}$$

The initial state is defined as $x_{i,0} = 0.5i$, while the initial state estimate is initialized to $\hat{x}_{i,0} = 0$. The problem-dependent scaling matrices U^v_k, S^v_k and the coefficients utilized in computing the upper bound matrices α^v_k, β^v_k are selected properly. The covariance matrix of noises $w_{i,k}$ and $v_{i,k}$ is set to $q = 1$ and $r = 0.5$, respectively.

In the given graph, a total of N nodes are distributed randomly across the square $[0, 1.1] \times [0, 1.1]$. Nodes are linked if their distance falls below d.

The evaluation criterion employed for comparison is the root mean square error (RMSE):

$$RMSE_k = \sqrt{\frac{1}{MN} \sum_{m=1}^{M} \sum_{i=1}^{N} \left(x_{i,k} - \hat{x}_{i,k}\,(m) \right)^2} \tag{28}$$

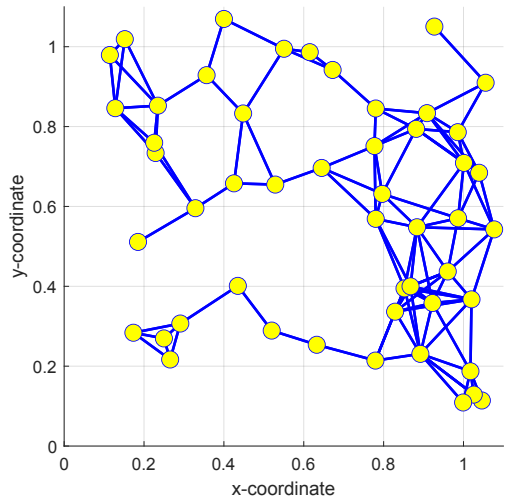

Fig. 2. Graph topology with $N = 50$.

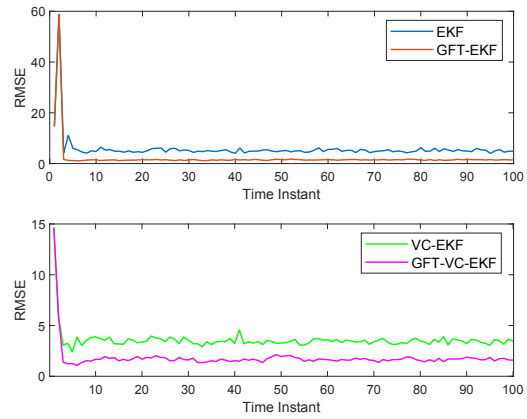

Fig. 3. RMSE with $N = 50$.

where $\hat{x}_{i,k}(m)$ represents the estimate from the mth Monte Carlo simulation, with a total of $M = 100$ independent Monte Carlo runs conducted.

Case 1: In this simulation, we set $d = 0.2$, and the number of nodes are selected as $N = 50, 100$, respectively. The communication relationship between the nodes in the graph and the RMSE comparison between filters in different topologies are shown in Figs. 2-5. It is evident that, the GFT-EKF exhibits better performance compared to the EKF, and the performance of the GFT-VC-EKF is superior to the VC-EKF. This highlights the considerable influence of the GFT approach on the improvement of filter performance for graphical nonlinear systems.

Case 2: The topological sparsity is an important index for graphical nonlinear systems. To verify the performance of the GFT-VC-EKF under different topological

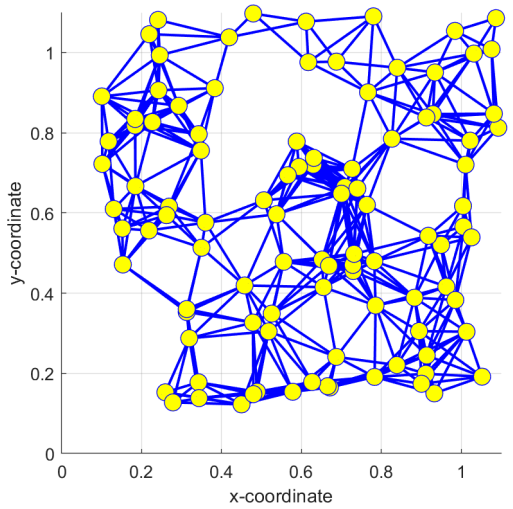

Fig. 4. Graph topology with $N = 100$.

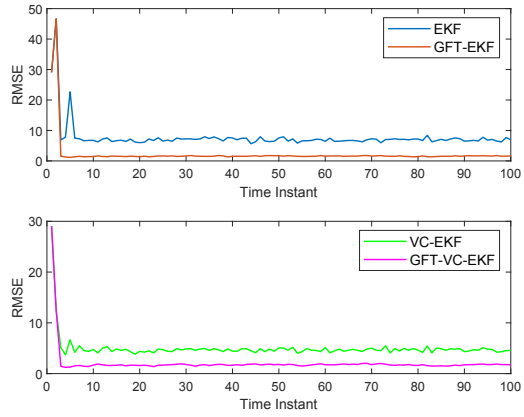

Fig. 5. RMSE with $N = 100$.

TABLE I
RMSE with different d and N.

d	Filter	$N = 25$	$N = 50$	$N = 75$	$N = 100$
0.2	EKF	4.38	5.76	6.89	7.71
	GFT-EKF	1.99	2.15	2.43	2.28
	VC-EKF	3.25	3.57	4.28	4.98
	GFT-VC-EKF	1.90	1.82	1.99	2.08
0.5	EKF	3.91	5.20	6.27	7.17
	GFT-EKF	1.98	2.02	2.05	2.18
	VC-EKF	3.09	3.82	2.25	2.36
	GFT-VC-EKF	1.91	2.01	1.92	2.05
0.8	EKF	3.87	4.94	6.08	6.73
	GFT-EKF	1.95	1.85	2.03	2.09
	VC-EKF	3.24	1.96	2.19	2.33
	GFT-VC-EKF	1.91	1.78	1.96	2.02

sparsity, we modify the connection distance d of the graph topology with the other parameters are the same as Case 1, and the corresponding RMSE are shown in Table I.

From Table I, it can be inferred that irrespective of the changes in topological sparsity, the GFT-VC-EKF consistently demonstrates superior performance compared to the other three filters. On the other hand, it can be seen from the limited data that, as the connection distance d increases, the filtering accuracy of EKF and GFT-EKF is improved, which means that the dense topology contributes positively to the enhancement of efficiency for the EKF and the GFT-EKF. For the VC-EKF and the GFT-VC-EKF, the impact of topological sparsity on them is not discussed here because their performance is affected by the selected parameters.

V. Conclusion

This paper has introduced an extended Kalman filter called GFT-VC-EKF with higher precision for graphical nonlinear systems. Inspired by the GFT, a diagonal Kalman gain matrix has been designed by using the eigenvector matrix of the Laplacian matrix. Then the upper bound for the predicted and updated error covariance matrices has been determined to address the presence of the unknown bounded matrix, so that the double guarantee of compensating for the linearization error and reducing the iterative cumulative error has been realized. The simulation results on a power system have shown that the GFT approach can play an active role in reducing the filtering error, and the proposed GFT-VC-EKF has superior performance. This paper has provided a new perspective on the filtering of graphical nonlinear systems whose node signals are one-dimensional, and our future work will consider the filtering of graphical systems with high-dimensional node signals.

References

[1] A. C. Yağan and M. T. Özgen, "Spectral graph based vertex-frequency Wiener filtering for image and graph signal denoising," IEEE Transactions on Signal and Information Processing over Networks, vol. 6, pp. 226–240, 2020.

[2] Y. He and H.-T. Wai, "Detecting central nodes from low-rank excited graph signals via structured factor analysis," IEEE Transactions on Signal Processing, vol. 70, pp. 2416–2430, 2022.

[3] W. Huang, A. G. Marques, and A. Ribeiro, "Collaborative filtering via graph signal processing," in 2017 25th European Signal Processing Conference (EUSIPCO), 2017, pp. 1094–1098.

[4] S.-P. Hsu, "On a class of controllable single-leader multi-agent systems," in 2016 European Control Conference (ECC), 2016, pp. 1874–1879.

[5] T. M. D. Tran and A. Y. Kibangou, "Consensus-based distributed estimation of Laplacian eigenvalues of undirected graphs," in 2013 European Control Conference (ECC), 2013, pp. 227–232.

[6] D. B. Tay, "Filter design for two-channel filter banks on directed bipartite graphs," IEEE Signal Processing Letters, vol. 27, pp. 2094–2098, 2020.

[7] Z. Xiao, H. Fang, and X. Wang, "Distributed nonlinear polynomial graph filter and its output graph spectrum: Filter analysis and design," IEEE Transactions on Signal Processing, vol. 69, pp. 1725–1739, 2021.

[8] T. M. Roddenberry, F. Gama, R. G. Baraniuk, and S. Segarra, "On local distributions in graph signal processing," IEEE Transactions on Signal Processing, vol. 70, pp. 5564–5577, 2022.

[9] A. Ortega, P. Frossard, J. Kovačević, J. M. F. Moura, and P. Vandergheynst, "Graph signal processing: Overview, challenges, and applications," Proceedings of the IEEE, vol. 106, no. 5, pp. 808–828, 2018.

[10] A. Sandryhaila and J. M. F. Moura, "Discrete signal processing on graphs," IEEE Transactions on Signal Processing, vol. 61, no. 7, pp. 1644–1656, 2013.

[11] C. Ozturk, H. M. Ozaktas, S. Gezici, and A. Koç, "Optimal fractional Fourier filtering for graph signals," IEEE Transactions on Signal Processing, vol. 69, pp. 2902–2912, 2021.

[12] K.-S. Lu, A. Ortega, D. Mukherjee, and Y. Chen, "DCT and DST filtering with sparse graph operators," IEEE Transactions on Signal Processing, vol. 70, pp. 1641–1656, 2022.

[13] S. Segarra, A. G. Marques, and A. Ribeiro, "Optimal graph-filter design and applications to distributed linear network operators," IEEE Transactions on Signal Processing, vol. 65, no. 15, pp. 4117–4131, 2017.

[14] G. Dehghani and H. Morady, "An algorithm for visibility graph recognition on planar graphs," in 2009 International Conference on Future Computer and Communication, 2009, pp. 518–521.

[15] A. Sandryhaila and J. M. F. Moura, "Discrete signal processing on graphs: Graph Fourier transform," in 2013 IEEE International Conference on Acoustics, Speech and Signal Processing, 2013, pp. 6167–6170.

[16] W. Li, X. Fu, B. Zhang, and Y. Liu, "Unscented Kalman filter of graph signals," Automatica, vol. 148, p. 110796, 2023.

[17] G. Sagi, N. Shlezinger, and T. Routtenberg, "Extended Kalman filter for graph signals in nonlinear dynamic systems," in ICASSP 2023-2023 IEEE International Conference on Acoustics, Speech and Signal Processing (ICASSP). IEEE, 2023, pp. 1–5.

[18] L. Xie, Y. C. Soh, and C. E. De Souza, "Robust Kalman filtering for uncertain discrete-time systems," IEEE Transactions on Automatic Control, vol. 39, no. 6, pp. 1310–1314, 1994.

[19] Y. Theodor and U. Shaked, "Robust discrete-time minimum-variance filtering," IEEE Transactions on Signal Processing, vol. 44, no. 2, pp. 181–189, 1996.

[20] G. Calafiore, "Reliable localization using set-valued nonlinear filters," IEEE Transactions on Systems, Man, and Cybernetics - Part A: Systems and Humans, vol. 35, no. 2, pp. 189–197, 2005.

[21] H. Ren, Z. Cheng, J. Qin, and R. Lu, "Deception attacks on event-triggered distributed consensus estimation for nonlinear systems," Automatica, vol. 154, p. 111100, 2023.

[22] J. Hu, Z. Wang, S. Liu, and H. Gao, "A variance-constrained approach to recursive state estimation for time-varying complex networks with missing measurements," Automatica, vol. 64, pp. 155–162, 2016.

[23] W. Li, Y. Jia, and J. Du, "Variance-constrained state estimation for nonlinearly coupled complex networks," IEEE Transactions on Cybernetics, vol. 48, no. 2, pp. 818–824, 2018.

[24] S. Kanna, D. H. Dini, Y. Xia, S. Y. Hui, and D. P. Mandic, "Distributed widely linear Kalman filtering for frequency estimation in power networks," IEEE Transactions on Signal and Information Processing over Networks, vol. 1, no. 1, pp. 45–57, 2015.

[25] G. Sagi and T. Routtenberg. (2022) GSP-based MAP estimation of graph signals. [Online]. Available: https://arxiv.org/abs/2209.11638

[26] A. Abur and A. G. Exposito, Power System State Estimation: Theory and Implementation. New York, NY, USA: Marcel Dekker, 2004.

[27] S. Grotas, Y. Yakoby, I. Gera, and T. Routtenberg, "Power systems topology and state estimation by graph blind source separation," IEEE Transactions on Signal Processing, vol. 67, no. 8, pp. 2036–2051, 2019.